Arab Gulf Journal of Scientific Research, 21 (1), pp 28 - 47 (2003)

ORIGIONAL PAPER

A A Ammar, E M Abdelrahman, H I Hassanein and K S Soliman

Radiometric Lithologic Interpretation of Aerial Radiospectrometric False Colour Image Maps, Eastern Desert, Egypt

Abstract: The area studied, Gabal Um-Rabul, is located in the northern part of the Eastern Desert of Egypt. It is covered by different varieties of rock formations, including successions of basement and sedimentary rocks. The contact zone between them is considered as an unconformity contact.

The area under consideration was included in an airborne gamma-ray spectrometric survey which was conducted by the Aero-Service Division, Western Geophysical Company of America in 1984. The present study deals with the interpretation of these aeroradiospectrometric survey data, using conventional and modern statistical methods of analysis, in addition to reinvestigating the different mapped lithologies and considering them as interpreted radiometric lithologic (IRL) units.

In this study, the geological map of the area was considered as a base for the radiometric lithologic interpretation of the data. The correlation between aeroradiospectrometry and lithology was conducted in two ways: the first one took into consideration the original lithological units, while the latter took into account the IRL units.

The resultant interpreted radiolithologic unit (IRLU) map shows that, the study area contains four basement rock units and five sedimentary formations with various T.C. radiometric levels and different radio element concentrations.

Keywords: Rock formations, Um Rabul, Egypt, geology, map, radiometric, lithologic, interpretation.

التأويل الإشعاعي الصخري للخرائط الإشعاعية الطيفية التصويرية زائفة الألوان بالصحراء الشرقية لمصر

أحمد أبوبكر عمار ، السيد محمد عبدالرحمن،
حمدي إسماعيل السيد حسانين، خالد سليمان سليمان

المستخلص: تتغطى منطقة الدراسة، جبل أم رابول في الصحراء الشرقية الشمالية لمصر. بنوعيات متعددة من تكوينات الصخور، متضمنة تتابعات الصخور النارية والمتحولة والرسوبية. ويعتبر نطاق إلتماس بين صخور القاعدة والرسوبيات نطاقاً متخالفاً.

اشتمل المسح الإشعاعي الطيفي الجيمي، الذي قام به قسم الخدمات الجوية (إيروسيرفيس)، التابع للشركة الجيوفيزيائية الغربية لأمريكا عام 1984م، منطقة الدراسة. بعد رسم الخرائط التصويرية زائفة الألوان، تتعامل الدراسة الحالية مع تأويل هذه المعطيات الإشعاعية الطيفية بإستخدام طرق التحليل الإحصائي التقليدية والحديثة، هذا بالإضافة إلى إعادة التحقق من تكوينات الصخور المتنوعة، وإعتبارها وحدات إشعاعية صخرية مؤولة.

مع اعتبار الخريطة الجيولوجية للمنطقة أساساً ومنطلقاً للتأويل الإشعاعي الصخري للمعطيات، تم إجراء إرتباط متبادل بين الوحدات الصخرية والقياسات الإشعاعية الطيفية بطريقتين: الأولي، أخذت بعين الإعتبار الوحدات الصخرية الأصلية، والأخري أدخلت في الحساب، الوحدات الإشعاعية الصخرية المؤولة.

أوضحت خريطة الوحدات الإشعاعية الصخرية المؤولة إحتواء منطقة الدراسة على أربع وحدات لصخور القاعدة، وخمس وحدات للتكوينات الرسوبية، ذات مستويات إشعاعية كلية مختلفة، وكذلك تركيزات للعناصر الإشعاعية الثلاثة.

كلمات مدخلية: تكوينات صخور، أم رابول، مصر، جيولوجيا، خرائط، قياس إشعاعي، تحليل.

Introduction

The area studied, Gabal Um-Rabul, is located in the northern part of the Eastern Desert of Egypt (Fig. 1). The area is bounded by latitudes 28° 07′ 30″ N and 28° 27′ 30″ N, and longitudes 32° 20′ E and 32° 50′ E. It is situated near the western coast of the Gulf of Suez region, west of Ras Gharib town.

The area under consideration is covered by different varieties of rock formations, consisting of igneous and metamorphic rocks eastwards as well as sedimentary rocks westwards. The igneous and metamorphic rocks represent a part of the northern basement of Egypt, which is a part of the Arabian – Nubian shield. The contact zone between the basement rocks and sedimentary successions is considered as an unconformity contact. The general topography of the eastern part of the area under consideration is more rugged than its western part. In addition, it includes a part of Red Sea plain to the east. It is generally dissected by several NE-, ENE-, NW-, and E-W trending wadis (dry valleys), which are mainly structurally controlled.

Ahmed A. Ammar
Nuclear Materials Authority, Exploration Division,
P.O. Box. 530, El-Maadi,
Cairo, Egypt.

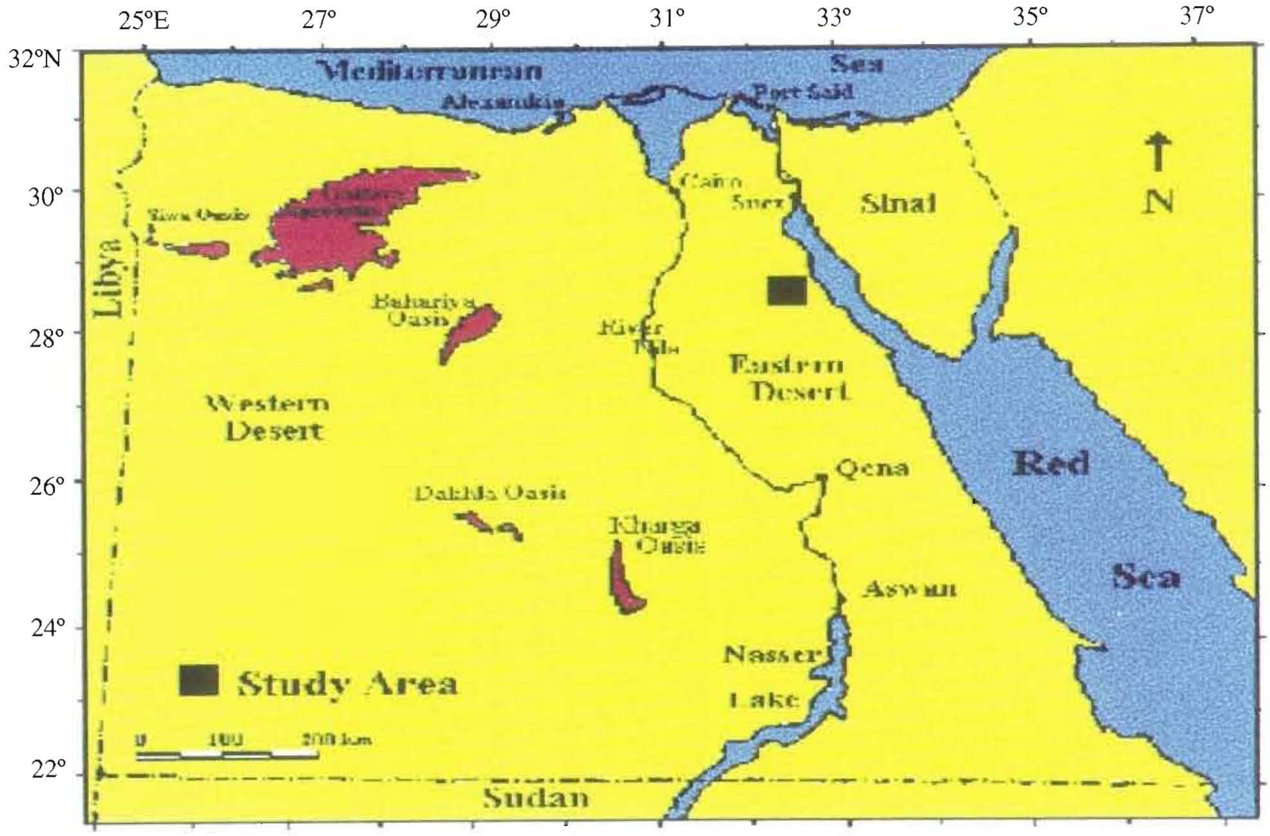

Fig. 1 Map of Egypt showing the location of Gabal Um-Rabul area, Northern Eastern Desert

Since mid-1967, high-sensitivity airborne gamma-ray spectrometry has been applied extensively in support of geological (lithological and structural) mapping and mineral exploration, especially in regions where the geology is complex, or the access is difficult. The method depends upon the fact that the measured absolute and relative concentrations of the radio elements potassium, uranium and thorium vary significantly with lithology (Darnley and Ford, 1989).

Darnley and Grasty (1971) have shown that the gamma-ray spectrometric "signatures" of rocks can be used to delineate the lithology and structure. Killeen (1979) stated that the concentrations of potassium, uranium and thorium in igneous rocks, all increase in overall abundance with increasing silica content up to and including the pegmatite phase. In a similar manner, they increase with increasing differentiation index. In sedimentary rocks, uranium tends to be concentrated in shales, particularly in the bituminous, carbonaceous and phosphatic types. In sandstones and other psammitic rocks, an increase in the uranium content is noticeable along with an increase in resistant minerals such as biotite, monazite, allanite and zircon. The uranium content of metamorphic rocks is generally of the same order of magnitude as their unmetamorphosed equivalents (IAEA, 1988).

The texture of aeroradiometric contours and their radiometric signatures could be an identification and an aid in the course of interpretation of the surface geology. Consequently, it is possible to identify lithological boundaries from the overall changes in the levels of radiation shown on the contour maps. The degree of this identification could be either obvious or vague depending upon the contrast in the radiometric signatures of the two adjacent rock units. Faults, shears, and certain lithological contacts may be manifested by disruption of the contours on the aeroradiometric map. Furthermore, faults sometimes exhibit radioactive highs due to increased permeability allowing access to migrating radon; other faults exhibit radioactive lows because of increased leaching of radioactive minerals along fault zones. In addition, linear trends may indicate strikes of sedimentary or metamorphic lithology and folds can be remarked by the disruption of the linear radiometric features that originate from a particular geological horizon (El-Sadek, 1998).

The investigated area was included in an airborne gamma-ray spectrometric survey, which was conducted by the Aero-Service Division, Western Geophysical Company of America, in 1984, for the Egyptian Geological Survey and Mining Authority (EGSMA), and the Egyptian General Petroleum Corporation (EGPC), Aero-Service, 1984. The present study deals with the interpretation of these aeroradiospectrometric survey data using conventional statistical methods of analysis, reinvestigating the different mapped lithological units, and regarding them as interpreted radiometric lithologic (IRL) units. This study was carried out through the following steps:

Analysis of the airborne gamma-ray spectrometric survey data by applying various statistical methods of analysis. These analyses could serve in the field of lithological mapping.

Definition and delineation of the interpreted radiolithologic units (IRLU) and subunits (IRLSU). Geochemical correction and modification of some contacts of the already-mapped lithological units.

Geological Setting

The area under study is included in the project of the Egyptian General Petroleum Corporation (EGPC) and Continental Oil Company (CONOCO). They published a new and updated geological map of Egypt, in 20 sheets, at a scale of 1:500,000 (Klitzsch *et al.* 1986 and 1987). The area under investigation is represented in Sheet No. (NH36SW, Beni Suef, CONOCO, 1987). Figure 2 shows the exposed rocks in the area studied, Gabal Um-Rabul, Northern Eastern Desert, Egypt. The rocks are grouped according to their modes of occurrence and their mutual relationships in the following sequence.

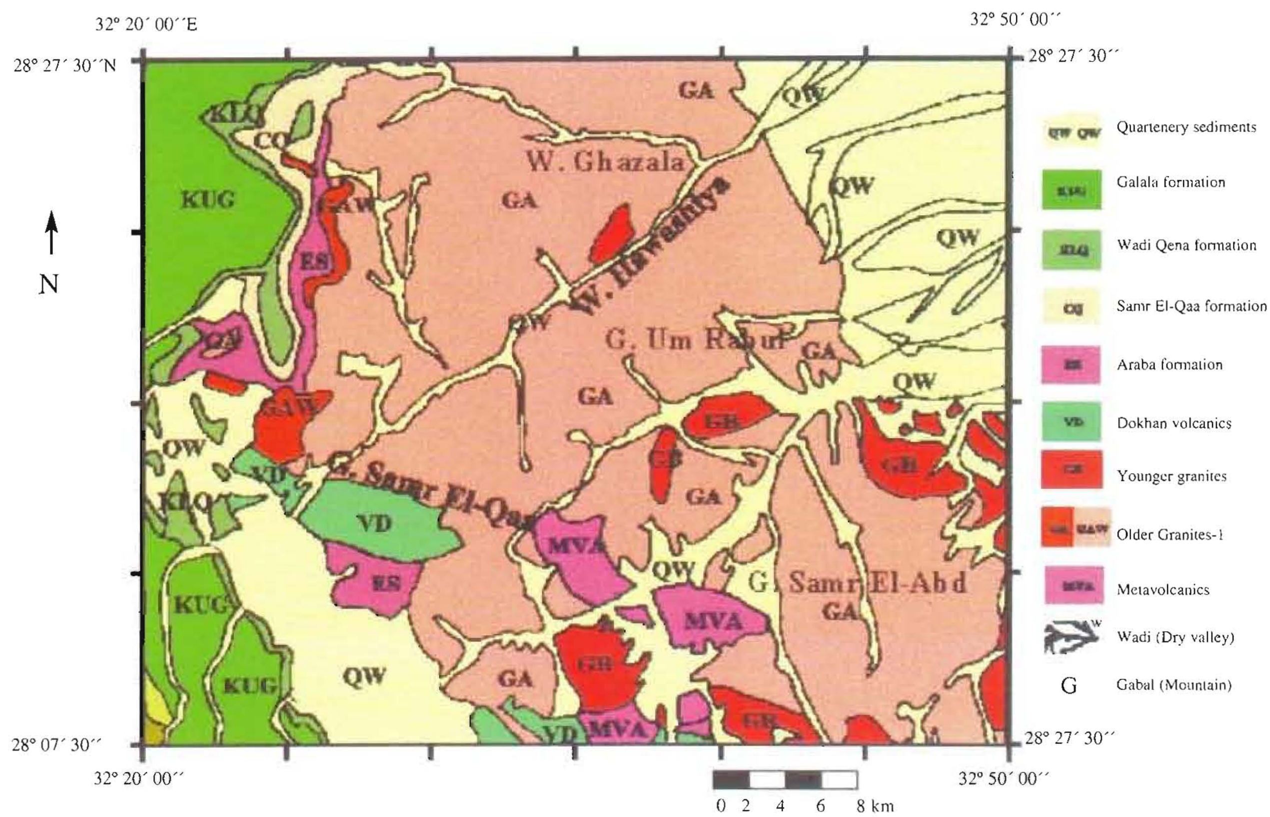

Fig. 2: Geological map of Gabal Um-Rabul area, Northern Eastern Desert, Egypt (after CONOCO, 1987).

1. Basement Rocks

1.1. Metagabbro to Metadiorite

These two types of rocks are represented in the southeastern part of the area under study. They are considered as intrusive rocks in the geosynclinal metasediments and metavolcanics (CONOCO, 1989). They are subdivided according to rock type into:

a - Intrusive metagabbro to metadiorite
b - Ophiolitic metagabbro
c - Metagabbro to metadiorite, undifferentiated

1.2. Metavolcanics

These rocks were interpreted as the product of volcanic activity during the subsidence phase of eugeosyncline (El-Ramly and Akkad, 1960). The metavolcanics are subdivided into three classes:

a - Intermediate to acidic metavolcanics and metapyroclastics
b - Ophiolitic metavolcanics
c - Metavolcanics, undifferentiated

1.3. Grelated Rocks

Late Proterozoic and younger granites occupy wide areas in the Northern Eastern Desert and Sinai of Egypt. They are subdivided according to rock type into

a- Calc-alkaline granites, comprising Ga(GA) and Gb(GB) granites. Ga(GA) granites correspond to "grey, older and Synorogenic granitoids" in previous classifications. They range in composition from quartz diorite to granodiorite and locally to monzogranite. Gb(GB) granites correspond to pink or younger granites in previous classifications.

b - Subalkaline to peralkaline granites and quartz syenites grouped together as G(g) granites. They are not represented in the area under study.

1.4. Dokhan Volcanics

Typical sequences of this rock unit are composed of intermediate to acidic volcanic rocks with their pyroclastic equivalents.

2 - Sedimentary Rocks

Sedimentary rocks are represented in the area under investigation in its western part. The oldest sedimentary rock in the area occurs at the western periphery of the basement complex. Table 1 shows the stratigraphic succession of the sedimentary rocks from the east to west (CONOCO, 1989).

Table 1. The stratigraphic succession of the sedimentary rocks from the east to west, Gabal Um-Rabul area, Northern Eastern Desert, Egypt; the oldest formation is at the bottom (CONOCO, 1989)

Stratigraphic succession	Age
Quaternary (QW) Formation	Quaternery
Galala(KUG) Formation	Cenomanian-Early Turonian
Wadi Qena (KLQ) Formation	Albian to Cenomanian
Samr El-Qaa (CQ) Formation	Carboniferous
Araba (ES) Formation	Cambrian

Aeroradiospectrometric Survey and Data Presentation

In 1984, through a contract between EGPC (the Egyptian General Petroleum Corporation) and EGSMA (the Egyptian Geological Survey and Mining Authority) and Aero-Service Division, Western Geophysical Company of America, USA; the latter carried out aeroradiospectrometric and aeromagnetic surveys for most of the surface area of the Eastern Desert of Egypt.

The aeroradiospectrometric survey was conducted along parallel flight lines oriented in a NE-SW direction at 1.5 km spacing. A highly sensitive airborne gamma-ray spectrometer (AGRS) system with 256-channels was used in gamma-ray spectrometric measurements. The altitude of the airplane during the survey was nearly 120 m (Aero-Service, 1984). The data were corrected and plotted as aeroradiospectrometric contour maps and profiles. In the present study, the digitizing process follows the basic acquired analog profiles of the flight lines drawn on the map of flight lines of the study area. Duval (1983) used the computer colour image technique in the interpretation of aerial gamma-ray spectrometric survey data. Consequently, the digitized total-count (T. C.) radiometry as well as potassium, uranium and thorium contents were plotted in the form of filled – colour image maps (Fig. 3, 4, 5 & 6).

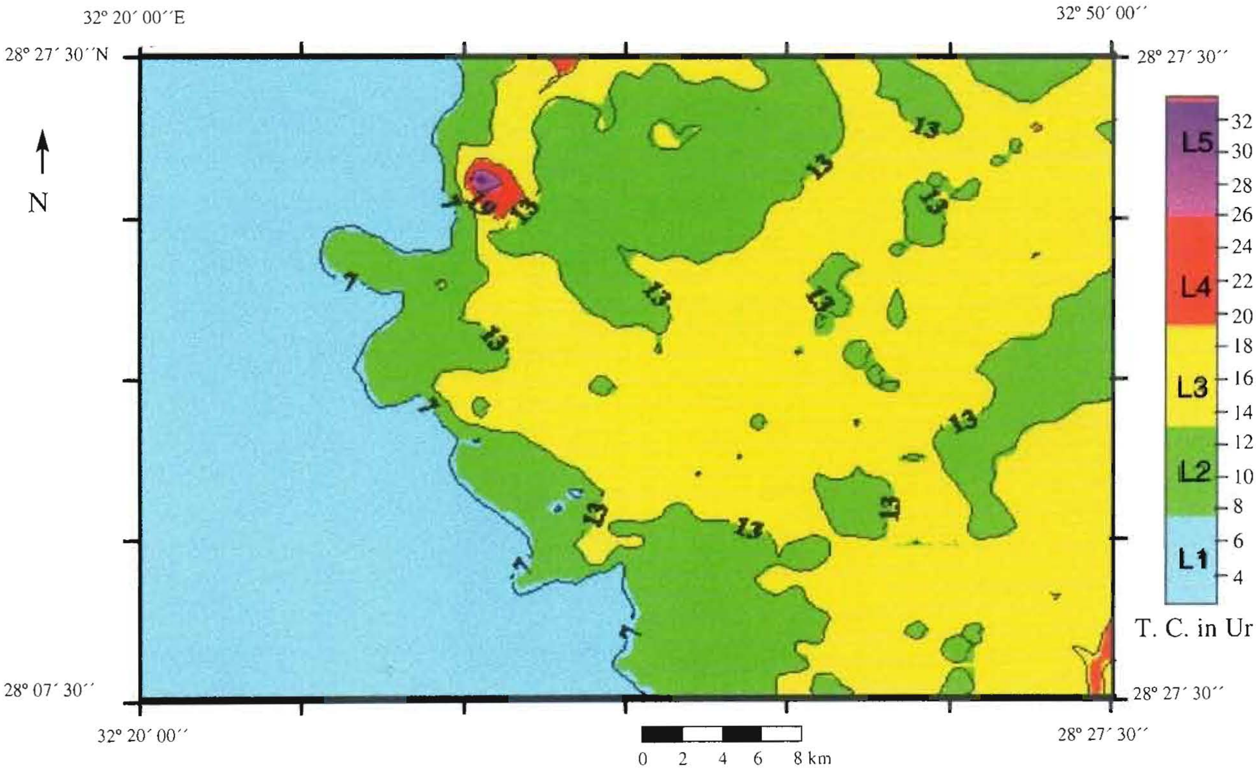

Fig. 3: Filled-colour image map of the aerial total-count (T.C.) radiometric survey data, Gabal Um Rabul area, Northern Eastern Desert, Egypt.

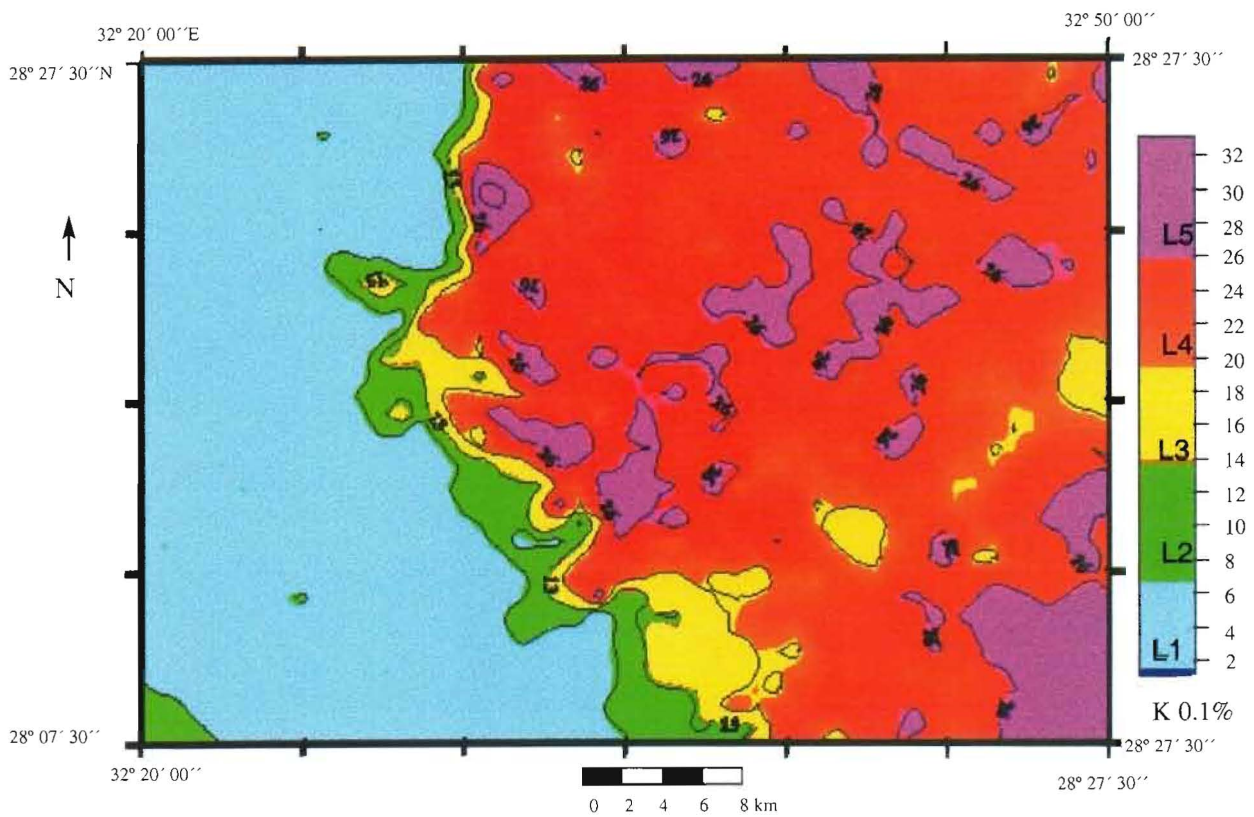

Fig. 4: Filled-colour image map of aerial spectral radiometric potassium (K), Gabal Um-Rabul area, Northern Eastern Desert, Egypt.

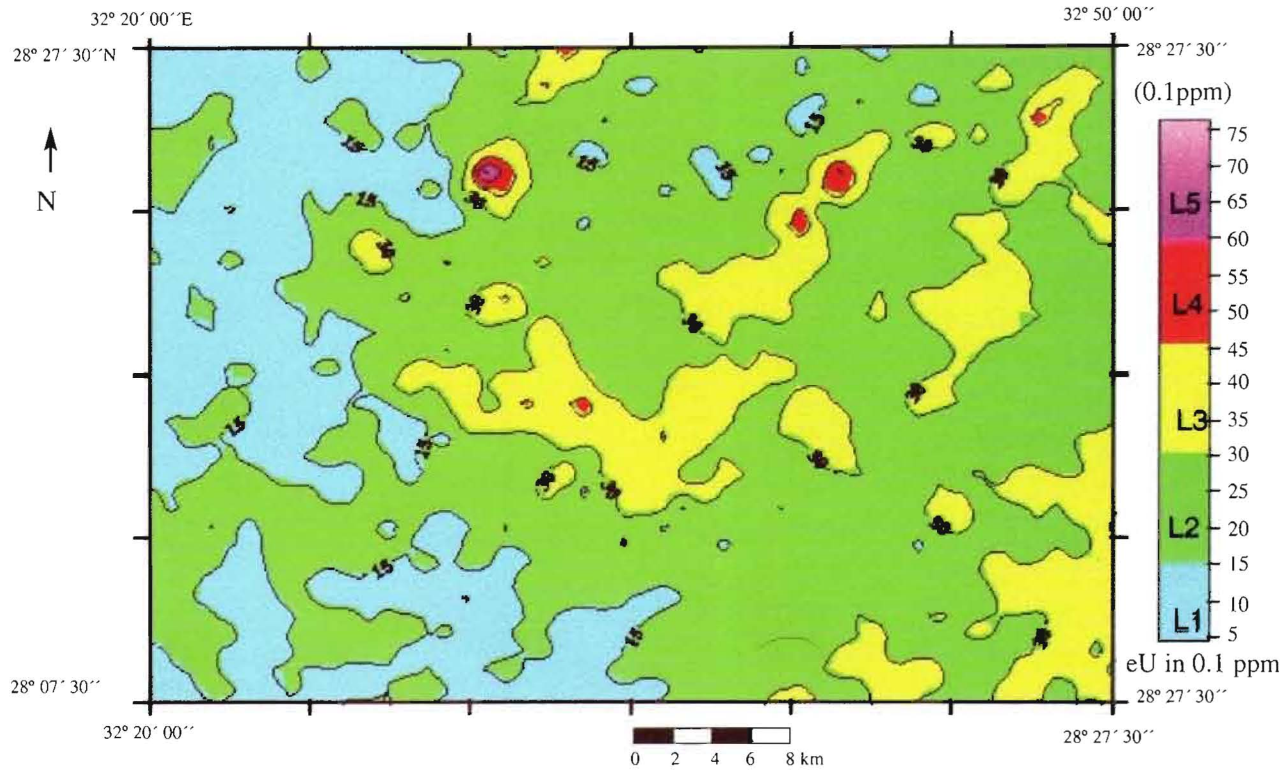

Fig. 5: Filled-colour image map of aerial spectral radiometric equivalent uranium (eU), Gabal Um-Rabul area, Northern Eastern Desert, Egypt.

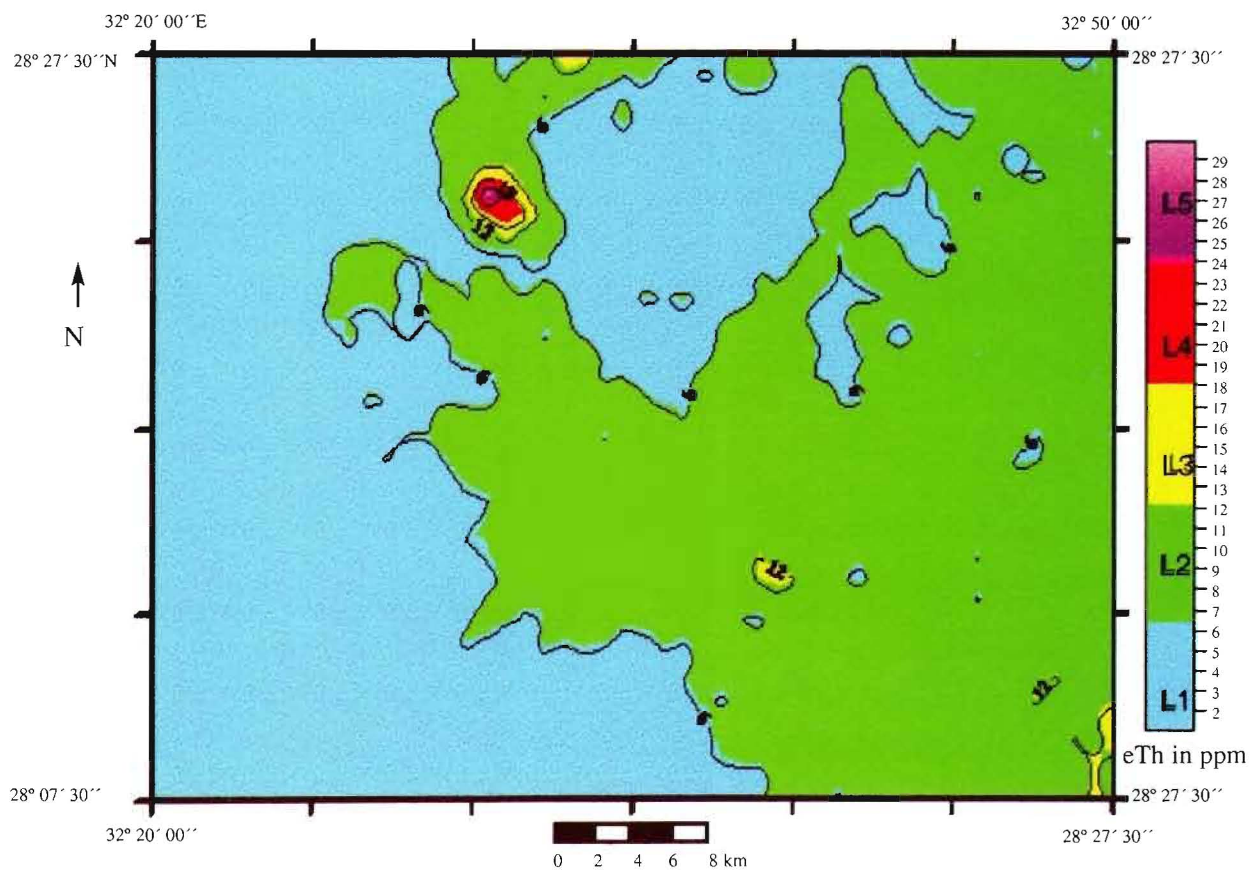

Fig. 6: Filled-colour image map of aerial spectral radiometric equivalent thorium (eTh), Gabal Um-Rabul area, Northern Eastern Desert, Egypt.

Statistical Analysis Techniques of Aeroradio-Spectrometric Survey Data

The techniques of statistical analysis are applied in the field of aerial radiospectrometry to determine the radiospectrometric background of the separate rock lithologic units of every type, guide the operations of exploration of radioactive mineralizations, permit the radiospectrometric (geochemical) delineation of boundaries between various kinds of rocks and assist the interpretation of geology, i.e., lithology and structure (Ammar *et al.* 1982). In addition, it is applied in order to get more accurate geochemical boundaries for the corresponding geologic units, obtain more significant information about the economic potentialities of the radioactive mineralized zones, and determine whether or not a statistically significant difference exists between the computed statistics possessed by the different rock units and formations, i.e., normal populations (IAEA, 1988).

The statistical analysis methods depend on testing the homogeneity of total-count (T.C.) aeroradiometric data of the study area as a whole and for each lithologic unit separately. Two types of homogeneity tests were used, the first is the chi-square (c^2) and the other is the normal probability plot. The normal probability plot consists of an arithmetic (interval) horizontal axis scaled for the data and a vertical axis so scaled that the cumulative distribution function of a normal distribution plot behaves as a straight (reference) line. The closer the data are to the reference line, the more likely they follow a normal distribution (Morris, 1985)

Mainly, the study area contains four basement groups: metavolcanics, older granites, younger granites, and Dokhan volcanics. It also includes five sedimentary formations: Araba, Samr El-Qaa, Wadi Qena, Galala, and Quaternary (see Fig. 2). Different symbols were chosen to identify various rock types exposed in the area under study. They are represented by two capital letters, e.g., QW for Quaternary sediments, VD for Dokhan volcanics, GA for older granites ...etc. Meanwhile, the Arabic numerals 1, 2, 3, ...etc, were used to denote a sequential arrangement for the different lithological units belonging to each rock type, e.g., VD-1 denotes the first rock unit (1) of the group of Dokhan volcanics (VD). Moreover, when the rock unit shows no normal distribution of measurements and has been subjected to subdivision, then another capital letter is added to denote this rock subunit, e.g., GA-1B for the second subunit (B) of the first unit (1) of the group of older granites (GA).

Accordingly, the whole T.C. aeroradiometric survey data were analyzed to test their homogeneity all over the study area. This analysis showed that the data are not normally distributed (Fig. 7a & Table 2). Consequently, the area under study was classified according to its geology into a number of geologic (lithologic) units. The T. C. aero-radiometric data, which correspond to each of these lithologic units, were picked up. Statistical analysis was carried out for testing their homogeneity. Consequently, the area under study was divided into a number of interpreted radiometric lithologic (IRL) units, each of which is characterized by a definite range and level of aerial radioactivity, arithmetic mean (X), and standard deviation (S). The normality of each IRL unit was defined from the chi - square (χ^2) test, and the normal probability plot (Table 2 and Fig. 7b — 7n). Testing of the different statistical hypotheses on different relationships that might exist between various IRL units of each rock group was conducted. This step was achieved through the application of four statistical inference tests: the Bartlett's for the homogeneity of variances, the analysis of variance (ANOVA) for the homogeneity of arithmetic mean (Table 3), the Fisher's (F-) test for the comparison of two variances, and the Student's (t-) test for the comparison of two arithmetic means (Table 4). These four tests were applied to the normally distributed IRL units of every rock group to see whether they are drawn from one and the same parent population or not (Mendenhall, and Sincich, 1992). Figures 8 and 9 show the normal probability plots of the aerial T.C. radiometric data of the different interpreted basement and sedimentary units.

Table 2: Summary of the statistical airborne total count T.C. radiometric characteristics of the IRL units, Gabal Um Rabul area, Northern Eastern Desert, Egypt.

IRL Unit	No.	Min.	Max.	$\overline{X}$	S	χ^2-test			Dist.	
			In Ur			Calc.	D.F.	Crit.	χ^2	NPP
The whole aerial radiometric data										
All area	1900	2.3	33.5	10.3	4.8	667.6	4	9.5	NN	NN
Metavolcanics (MVA)										
MVA-1	18	7.4	13.	4 9.	4 2.0	-	-	-	-	NN
MVA-2	16	10.9	14.6	13.0	1.0	-	-	-	-	N
MVA-3	20	8.7	17.5	13.4	2.4	-	-	-	-	N
Older (grey) granites										
GA-1	556	2.9	33.5	11.5	4.1	83.9	2	6.0	NN	NN
GA-1A	58	3.1	4.5	3.9	0.4	2.1	3	7.8	N	N
GA-1B	92	4.6	9.9	7.2	1.5	8.5	5	11.0	N	N
GA-1C	379	10.8	17.42	13.4	1.5	4.8	3	7.8	N	N
GA-2	12	11.9	14.98	13.5	1.1	-	-	-	-	NN
GA-3	145	10.8	20.01	14.7	1.9	1.4	1	3.8	N	N
GA-4	40	12.3	16.52	14.7	1.2	3.7	3	7.8	N	N
Younger (pink) granites (GB)										
GB-1	18	11.9	18.21	14.5	1.9	-	-	-	-	N
GB-2	12	8.1	10.80	9.4	1.0	-	-	-	-	N
GB-3	14	12.1	17.58	14.6	1.4	-	-	-	-	NN
GB-4	32	10.1	18.14	13.5	2.2	2.1	2	6.0	N	N
Weathered granites and syenites (GAW)										
GAW-1	14	2.5	5.0	4.2	0.7	-	- -	-		NN
GAW-2	8	3.2	11.96	6.0	3.0	-	-	-	-	NN
Dokhan volcanics (VD)										
VD-1	16	3.8	7.9	5.5	1.6	-	-	-	-	NN
VD-2	25	4.2	5.6	4.7	0.4	-	-	-	-	N
Araba Formation (ES)										
ES-1	13	3.6	5.6	4.4	0.6	-	-	-	-	N
ES-2	19	3.2	5.1	4.1	0.6	-	-	-	-	N
Samr El-Qaa Formation (CQ)										
CQ	35	2.8	6.5	4.0	0.8	2.1	1	3.8	N	N
Wadi Qena Formation (KLQ)										
KLQ-1	11	3.5	6.5	4.6	0.8	-	-	- -	N	N
KLQ-2	20	2.7	5.6	3.6	1.1	-	-	-	-	N
KLQ-3	25	2.7	5.3	3.9	0.7	-	-	-	-	N
Galala Formation (KUG)										
KUG-1	56	2.7	6.4	4.5	0.7	2.3	1	3.8	N	N
KUG-2	100	2.3	5.0	3.6	0.6	0.3	2	6.0	N	N
Undifferentiated Quaternary sediments (QW)										
QW-1	122	2.8	6.6	4.4	0.7	2.5	2	6.0	N	N
QW-2	70	9.1	17.05	13.3	1.9	5.6	4	9.5	N	N
QW-3	235	3.2	19.90	11.3	4.6	191.10	5	11.1	NN	NN
QW-4	188	9.8	16.82	13.6	1.4	2.8	3	7.8	N	N

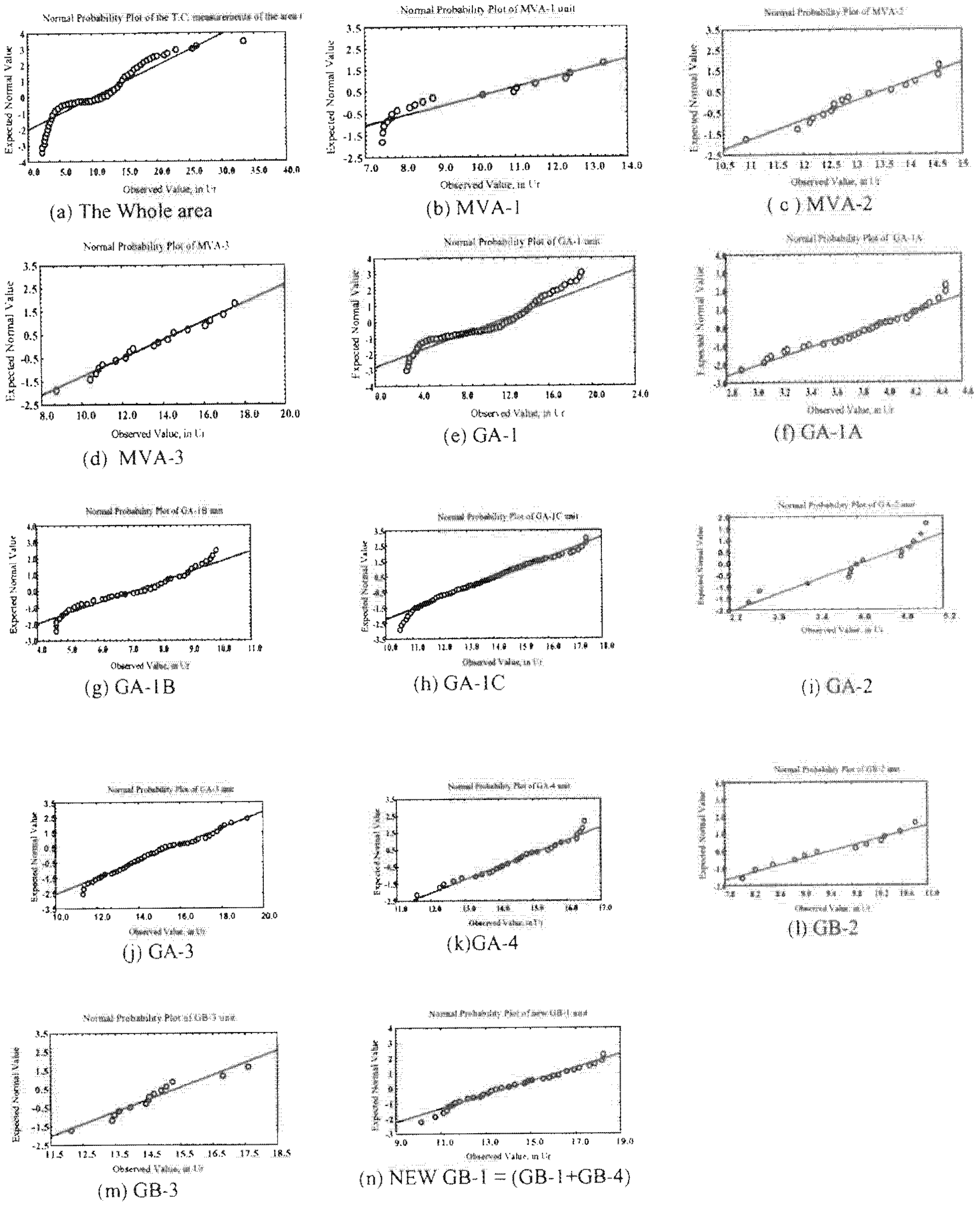

Fig. 7: Normal probability plots of the T.C. aeroradioactivity survey data of the whole area (a), metavolcanics, MVA-1 (b), MVA-2 (c) & MVA-3 (d), older granites, GA-1 (e), GA-1A (f), GA-1B (g), GA-1C (h), GA-2 (i), GA-3 (j) & GA-4 (k) and younger granites, NEW GB-1 (l), GB-2 (m), GB-3 (n), Gabal Um Rabul area, Northern Eastern Desert, Egypt.

Table 3: Results of the application of Bartlett's and ANOVA statistical inference tests for the aerial T.C. radiometric characteristics, Gabal-Um Rabul area, Northern Eastern Desert, Egypt.

Groups of IRL units	Bartlett's test		Result	ANOVA-test		Result
	Calc.	Crit.		Calc.	Crit.	
Older (grey) granites (Gα)						
GA-1A, GA-1B, GA-1C, GA-3 & GA-4	129.04	9.49	Rej.	-	-	-
GA-1A, GA-1B, GA-1C & GA-3	124.17	7.82	Rej.	-	-	-
GA-1A, GA-1B, GA-1C & GA-4	102.67	7.82	Rej.	-	-	-
GA-1A, GA-1B, GA-3 & GA-4	128.08	7.82	Rej.	-	-	-
GA-1A, GA-1C, GA-3 & GA-4	128.98	7.82	Rej.	-	-	-
GA-1B, GA-1C, GA-3 & GA-4	21.91	7.82	Rej.	-	-	-
GA-1A, GA-1B & GA-4	10.95	5.99	Rej.	-	-	-
GA-1A, GA-1B & GA-3	122.06	5.99	Rej.	-	-	-
GA-1B, GA-1C & GA-3	15.51	5.99	Rej.	-	-	-
GA-1B, GA-1C & GA-4	4.04	5.99	Acc.	498.8	3.01	Rej.
GA-1B, GA-3 & GA-4	15.77	5.99	Rej.	-	-	-
Younger (pink) granites (Gβ)						
GB-1, GB-2 & GB-4	8.18	5.991	Rej.	-	-	-
Undifferentiated Quaternary sediments (QW)						
QW-1,QW-2 & QW-4	99.13	5.99	Rej.	-	-	-

Table (4): Results of application of the Fisher's (F-) and Student's (t-) statistical inference tests for the airborne T.C. radiometric characteristics of the normal pairs of IRL units, Gabal Um-Rabul area, Northern Eastern Desert, Egypt.

Pair ofIRL units	F-test		Result	t-test		Result
	Calc.	Crit.		Calc.	Crit.	
Metavolcanics (MVA)						
MVA-2 & MVA-3	5.29	2.23	Rej.	-	-	-
Older (grey) granites (Gα)						
GA-1A & GA-1B	16.26	1.50	Rej.	-	-	-
GA-1A & GA-1C	15.50	1.39	Rej.	-	-	-
GA-1A & GA-3	25.90	1.44	Rej.	-	-	-
GA-1A & GA-4	9.46	1.61	Rej.	-	-	-
GA-1B & GA-1C	1.04	1.30	Acc.	35.55	1.97	Rej.
GA-1B & GA-3	1.59	1.32	Rej.	-	-	-
GA-1B & GA-4	1.71	1.61	Rej.	-	-	-
GA-1C & GA-3	1.67	1.30	Rej.	-	-	-
GA-1C & GA-4	1.64	1.43	Rej.	-	-	-
GA-3 & GA-4	2.74	1.48	Rej.	-	-	-
Younger (pink) granites (Gβ)						
GB-1 & GB-2	4.08	2.37	Rej.	-	-	-
GB-1 & GB-4	1.30	1.94	Acc.	1.43	2.86	Acc.
GB-2 & GB-4	5.34	2.10	Rej.	-	-	-
Araba Formation (ES)						
ES-1 & ES-2	1.07	2.34	Acc.	1.56	2.05	Acc.
Wadi Qena Formation (KLQ)						
KLQ-2 & KLQ-3	1.01	2.04	Acc.	1.91	2.019	Acc.
Galala Formation (KUG)						
KUG-1 & KUG-2	1.73	1.49	Rej.	-	-	-
Undifferentiated Quaternary sediments (QW)						
QW-1 & QW-2	8.04	1.41	Rej.	-	-	-
QW-1 & QW-4	409.01	1.32	Rej.	-	-	-
QW-2 & QW-4	50.85	1.36	Rej.	-	-	-

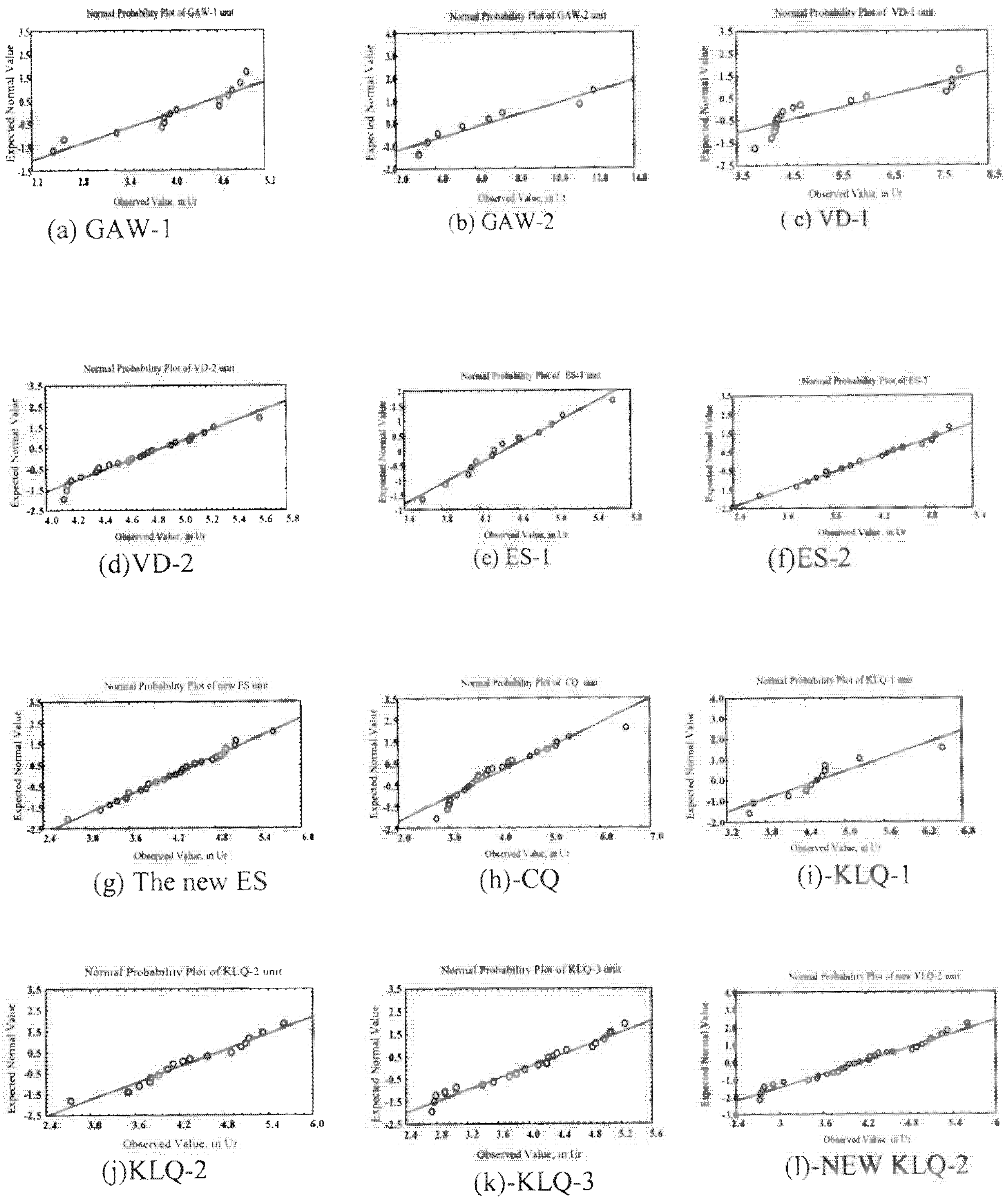

Fig. 8: Normal probability plots of the T.C. aeroradioactivity survey data of the weathered granites and Syenites subunits, GAW-1 (a) and GAW-2 (b), Dokhan volcanics subunits, VD-1 (c) & VD-2 (d), Araba Formation subunits, ES-1 (e), ES-2 (f) and the new ES unit (g), Samr El-Qaa Formation, CQ (h) and Wadi Qena Formation subunits, KLQ-1 (i), KLQ-2 (j), KLQ-3 (k) and the new KLQ-2 unit (l), Gabal Um Rabul area, Northern Eastern Desert, Egypt.

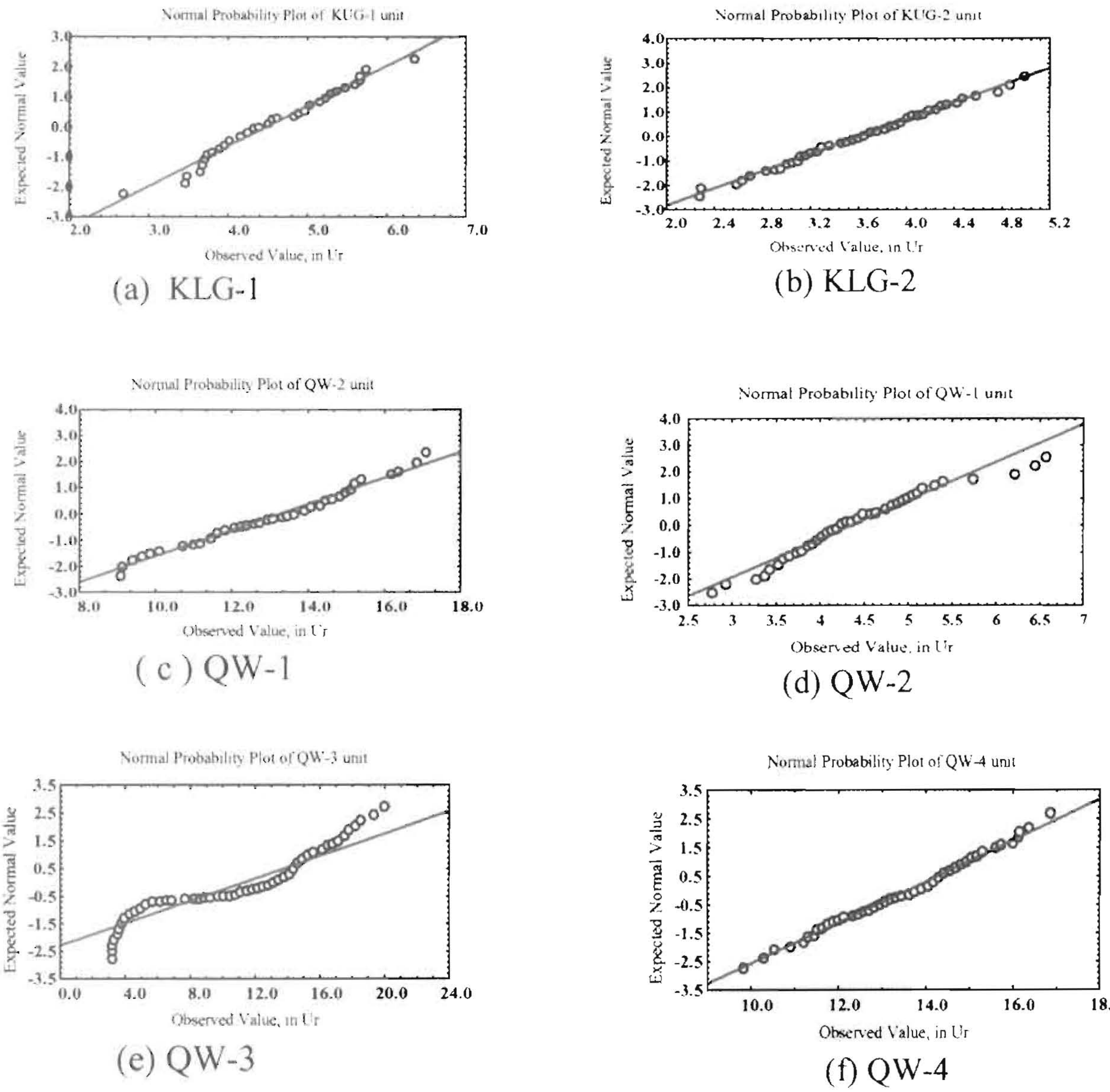

Fig. 9: Normal probability plots of the T.C. aeroradioactivity survey data of the Galala Formation subunits, KLG-1 (a) & KLG-2 (b) and the undifferentiated Quaternary sediments, QW-1 (c), QW-2 (d), QW-3 (e) and QW-4 (f), Gabal Um Rabul area, Northern Eastern Desert, Egypt.

Qualitative Interpretation of Aerial Gamma-Ray Spectrometric Data

Qualitative Interpretation

The four aerial spectral radiometric variable maps, total-count (T.C.), potassium (K), equivalent uranium (eU), and equivalent thorium (eTh), reveal different radiospectrometric levels registered over the study area (see Fig. 3 - 6).

The patterns of aerial radiospectrometry reflect much of the regional lithology, as well as many local changes in the regional trend of rocks that are marked by corresponding changes in the radiospectrometric levels. According to the colour variation which reflects the variation of each of the total-count, potassium, equivalent uranium and equivalent thorium filled-colour image maps (see Figs. 3, 4, 5 & 6), either individually or collectively, five main, relative and distinct levels ranging from very low to very high radiation were delineated visually to help in the radiometric lithologic interpretation. Delineation of these five general levels took into consideration neither the minute variation within these levels nor the roles of changes of the lithology and structure. The radiospectrometric boundaries between these five different and prominent levels were traced in accordance with the steep radiospectrometric gradients of the contour lines separating them. The exact and proper delineation and characterization will be dealt within the quantitative interpretation of these data where the role of geology will be effective and efficient. These five relative and distinct radiospectrometric levels could be described in the following.

1. Very low radiospectrometric level

This level is mainly encountered in the western part of the study area, from north to south. It coincides with the sedimentary section of the study area and varies from >0 to 6.5Ur in T.C. radioactivity, from >0 to 0.60% in K-content and from >0 to 1.5ppm in eU content and reaches to 6ppm in eTh content (see Fig. 3, 4, 5 & 6).

2. Low radiospectrometric level

For total-count (T.C.) radioactivity and potassium maps this low γ-ray spectrometric level coincides with the contact zone between the sedimentary and basement rocks, and varies from 7.0 to 13.0Ur for T. C. radioactivity (see Fig. 3) and from 0.6 to 1.3% for K-content (see Fig. 4). In both eU and eTh maps, this level is scattered all over the study area and has a vast areal distribution. It is met over the Galala formation, Araba formation, metavolcanics , Wadi Abu-Had older granites, as well as Wadi Hawashiya younger granites. This level generally varies in intensity from 1.50 to 3.0ppm for eU content (see Fig. 5) and from 12 to 18ppm for eTh content (see Fig. 6).

3. Intermediate radiospectrometric level

The total-count radioactivity of this intermediate γ-ray spectrometric level coincides with Quaternary sediments surrounding the contact zone between the sedimentary and basement rocks and varies in aerial radioactivity from 13.0 to 20Ur (see Fig. 3). Meanwhile, the intermediate potassium level is met also along the contact zone between the sedimentary and basement rocks as well as some spots in older granites, metavolcanics, and surrounding the main course of Wadi Abu-Had. It varies in intensity from 1.3 to 2.0% K (see Fig. 4).

This level on the eU map is met over some spots in older granites, north Wadi Hawashiya taking a NE-direction, over Gabal Um-Rabul, surrounding the main course of Wadi Abu-Had, as well as in the southeastern part of the study area. It varies in intensity from 3.0 to 4.5ppm eU (see Fig. 5). On the eTh map, this level is met over metavolcanics, the course of Wadi Abu-Had, older granites, parts surrounding the northeastern side of Wadi Hawashiya, as well as younger granites. It varies in intensity from 12.0 to 18.0ppm eTh (see Fig. 6).

4. High radiospectrometric level

This level is encountered as sporadic zones with different shapes distributed over older and younger granites. It also corresponds, in general, to the southeastern part of the study area, at equidistance between Gabal Um-Rabul and Gabal Samr El-Qaa, taking a NW-direction, as well as in the mid-northern part of the study area surrounding a significant zone of T. C. anomalous radioactivity. This level ranges in aerial T. C. radioactivity from 20.0 to 27.0Ur (see Fig. 3). The potassium high level is encountered as zones with different shapes distributed over older and younger granites. It mainly corresponds to the eastern part of the study area occupied by Precambrian basement rocks and ranges in intensity from 2.0 to 2.7% K (see Fig. 4). The eU high level is represented by separated zones with different shapes distributed over older and younger granites taking the trends of major wadis. It also surrounds the levels of very high eU intensity and ranges in intensity from 4.5 to 6.0ppm eU (see Fig. 5).

The eTh high level is met in the form of one spot in older granites, which surrounds a zone of eTh anomalous measurements, located between Gabal Um-Rabul and Gabal Samr El-Qaa, as well as in the southeastern part of the study area over younger granites. It varies in intensity from 18.0 to 24.0ppm eTh (see Fig. 6).

5. Very high radiospectrometric level

This very high γ-ray spectrometric level coincides only with one zone seen in the older granites. This zone is located approximately in the mid-northern part of the study area, to the east of the contact zone between the sedimentary and basement rocks and shows an aerial T.C-radiometric intensity attaining more than 27.0Ur (see Fig. 3). With respect to potassium, this very high level coincides with two zones on the older granites. These two zones are located in the mid-northern part of the study area, to the east of the contact zone between the sedimentary and basement rocks, as well as at its southeastern parts and show aerial intensities reaching more than 3.0% K (see Fig. 4).

On the eU map (see Fig.5), this very high level coincides with three zones on the older granites. The first zone is located in the mid-northern part of the study area, to the east of the contact between the sedimentary and basement rocks. The latter two zones are located near Wadi Hawashiya and take the general NE-direction with aerial eU intensities attaining more than 5.75ppm (see Fig. 5). Meanwhile, on the eTh map, this level coincides only with one zone on the older granites. This zone is located in the mid-northern part of the study area, to the east of the contact zone between the sedimentary and basement rocks. This zone has an aerial eTh intensity reaching more than 24.0 eTh (see Fig. 6).

The authors believe that this very high level occurs over younger granites rather than older granites and this represents an error in the geological mapping.

Quantitative Interpretation

The radiometric lithologic mapping was conducted for the whole area under study, which includes both basement and sedimentary rock units. The registered ranges of aerial T.C. radioactivity were found to vary from 2.27 to 33.49Ur, arithmetic means from 3.56 to 15.56Ur, and standard deviations from 0.37 to 4.61Ur (see Table 2). The testing of the homogeneity of the T.C. radiometric measurements recorded over the study area as a whole, the computed value of the (χ^2) test, and the normal probability plot (see Fig. 7a), all indicate that they are not homogeneous. This indicates that the area is not representing one lithologic unit as a whole, but contains different types of rock units, a conclusion that is true. All lithologic units and sub-lithologic units for the basement and sedimentary rocks will be discussed under the following headings.

Basement Rocks

Three main types of rocks, metavolcanics (MVA), granites and related rocks (GA,GB and GAW) and Dokhan volcanics (VD), were found to represent the basement rocks in the study area (see Fig. 2). Relatively, the average total-count radioactivity of the basement rocks is higher than that of the sedimentary rocks. In the following, a concise discussion of the distribution and characterization of the basement rock units of the area under study is presented.

Metavolcanics (MVA)

The metavolcanics in the area under study are located at Gabal Samr El-Abd (see Fig. 2). They are considered as intermediate metavolcanics, which are composed of intermediate to acidic metavolcanics and metapyroclastics. They are essentially composed of meta-andesite and metadacite together with subordinate amounts of metabasalt and metarhyolite (El-Ramly & Akkad, 1960).

As a result of the investigation of the total-count aeroradiometric map (see Fig. 3), the metavolcanics could be identified by their intermediate T.C level, which ranges from 7.4 to 17.5Ur. According to the geological map (see Fig. 2), the metavolcanics are exposed in three localities confined to the southern part of the study area. Their calculated arithmetic means range from 9.4 to 13.4Ur and their standard deviations vary from 1.0 to 2.4Ur (see Table 2).

As a result of the statistical analysis of the airborne total-count radiometric survey data, the metavolcanics were divided into three IRL units (MVA-1, MVA-2, and MVA-3, Fig. 10). The first IRL unit is the southern one and is coded as (MVA-1). The T.C. radiometric intensity measurements recorded from the air vary between 7.44 and 13.35Ur. The normal probability plot (see Fig. 7b) proves that this IRL unit, which lacks normal distribution, shows an arithmetic mean of 9.43Ur and a standard deviation of 2.08Ur (see Table 2).

The second IRL unit of metavolcanics is the eastern one and is coded as (MVA-2, Fig. 10). The registered T.C. aeroradiometric measurements range in intensity between 10.91 and 14.55Ur. Its radiometric measurements were statistically analyzed and the normal probability plot (see Fig. 7c) shows a normal distribution with an arithmetic mean of 12.97Ur and a standard deviation of 1.02Ur (see Table 2).

The third IRL unit metavolcanics is the western one and is coded as (MVA-3, Fig. 10). The T.C. aeroradiometric measurements range in intensity between 8.74 and 17.51Ur. The radiometric measurements were statistically analyzed and the normal probability plot (see Fig. 7d) indicates a homogeneous distribution with an arithmetic mean of 13.4Ur and a standard deviation of 2.4Ur (see Table 2).

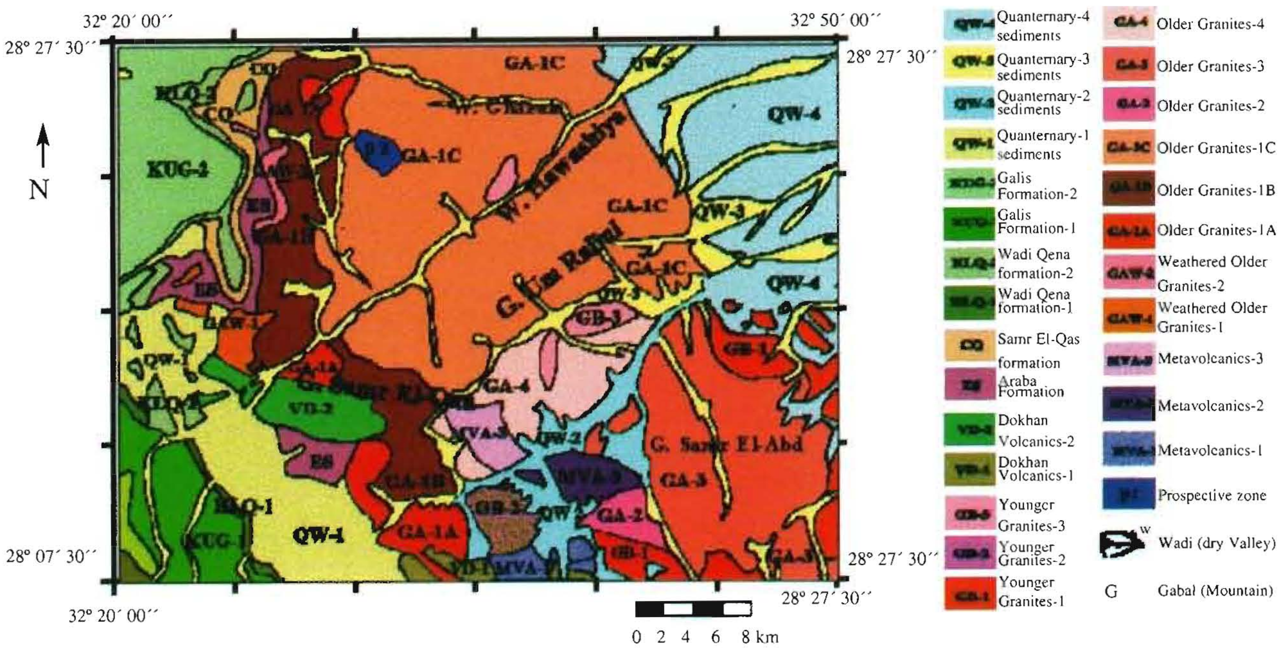

Fig. 10: Interpreted radiometric lithologic unit (IRLU) map, Gabal Um-Rabul area, Northern Eastern Desert, Egypt.

Statistical inference tests were applied to the two normal IRL units of metavolcanics coded as (MVA-2 and MVA-3) to see what relations may arise among them. This work was achieved by applying the Fisher's (F) and the Student's (t) tests for comparison of this pair of IRL units. The results of these two tests are organized in Table 4. From the results of the statistical inference tests, a conclusion could be reached that these two IRL units of metavolcanics could not be considered as belonging to one and the same parent population from the radioactivity point of view.

Granites and related rocks (GA, GB and GAW)

This group of rocks may represent the source of radioactive mineral deposits in the area under consideration. This group includes two types of granitic rocks: the first is the calc–alkaline granites (GA and GB) and the second is the subalkaline to peralkaline granites and quartz syenites (GAW).

Calc-alkaline granites, comprising older (GA) and younger (GB) granites

According to the geological map of the study area (see Fig. 2), the calc-alkaline granites includes two subgroups: older granites (GA) and younger granites (GB).

1. Older granites (GA)

Older granites are exposed in four localities coded as: GA-1, GA-2, GA-3 and GA-4. The normal probability plot of the GA-1 IRL unit (see Fig. 7e) and the chi-square value (see Table 2) reveal that the distribution of T.C. radioactivity of this IRL unit is not normal. Therefore, it could be divided into three subunits (GA-1A, GA-1B and GA-1C). The Chi-square values of these three subunits (see Table 2) and the normal probability plots (see Fig. 7f, 7g & 7h) prove that the distribution of the aerial T.C. radioactivity measurements of each submit is normal.

Consequently, the GA rock group was considered as representing three IRL sub-units: GA-1A, GA-1B, GA-1C, and three IRL units GA-2, GA-3 and GA-4. The normal probability plot (see Fig. 7i) and the chi-square value (see Table 2) prove that the distribution of T.C. radioactivity of the (GA-2) IRL unit is not normal, while GA-3 and GA-4 IRL units show normal distribution. In addition, it could be concluded that the two IRL units coded as GA-1A and GA-1B are of relatively low radioactivity levels, while the remaining four IRL subunits and units coded as GA-1C, GA-2, GA-3 and GA-4 are of relatively high to very high radioactivity levels.

Tables 3 and 4 show the results of statistical inference tests that were applied to see what relations may arise among the normal IRL units and subunits of GA rock group (GA-1A, GA-1B, GA-

1C, GA-3 and GA-4). From these results, it could be concluded that the various IRL units of older (GA) granites could not be considered as belonging to one and the same parent population as far as the T.C. aerial radioactivity is considered.

2. Younger granites (GB)

Younger granites are exposed in four localities of the study area coded as: GB-1, GB-2, GB-3 and GB-4 (see Fig. 2). The normal probability plot (see Fig. 7n) and the chi-square test values (see Table 2) prove that only the aerial T. C. radiometric measurements recorded over GB-3 IRL unit are not normally distributed.

Statistical inference tests were applied to see what relations may arise among the three various and normal IRL units of the younger (GB) pink granites (GB-1, GB- 2 and GB-4). GB-3 IRL unit was not included in these tests, because it proved to be abnormal. The results of inference tests are organized in Tables 3 and 4.

From the results of the statistical inference tests, it could be concluded that the two units (GB-1 and GB-4) could be considered as belonging to one and same parent population from the radioactivity point of view. The normal probability plot (see Fig. 7l) shows that this new GB-1 IRL unit of younger (GB) granites, which comes from adding the aeroradiometric measurements of GB-1 and GB-4, shows normal distribution as far as radioactivity is concerned.

Subalkaline to Peralkaline Granites and Quartz Syenites (GAW)

According to the geological map of the area under study, GAW granites and syenites are exposed in only two localities at the western periphery of the older (GA) grey granites, at the contact zone between the basement and sedimentary rocks (see Fig. 2). The total-count aerial radiometric survey data of each locality were statistically treated as two different IRL units (coded as GAW-1 and GAW-2). The normal probability plots (see Fig. 8a & 8b) and the chi-square test values reveal that the measurements registered over each of these two IRL units are not normally distributed (see Table 2) from the radioactivity point of view.

Dokhan Volcanics (VD)

According to the geological map (see Fig. 2), VD is exposed into only two localities at Gabal Samr El-Qaa and in the southern part of the study area. As a result of the application of the statistical methods of analysis on the aerial total-count radiometric survey data, the Dokhan volcanics are treated as two IRL units coded as VD-1 and VD-2 (see Fig. 10). The normal probability plot (see Fig. 8c) and the chi-square test value reveal that the measurements recorded over VD-1 IRL unit show abnormal distribution, while those registered over VD-2 (see Fig. 8d) IRL unit indicate normal distribution (see Table 2) as far as radioactivity is considered.

Sedimentary Rocks

Araba Formation (ES)

According to the geological map of the study area (see Fig. 2), the Araba Formation (ES) is exposed in two localities: one in the northwestern part and the other in the southwestern part of the study area. As a result of application of the statistical methods of analysis on the total-count aerial radiometric survey data, this formation was treated statistically as two IRL units, coded as ES-1 and ES-2 (see Fig. 10). The normal probability plot (see Fig. 8e & 8f) and the chi-square test values (see Table 2) reveal that the measurements recorded over ES-1 and ES-2 IRL units are characterized by normal distribution as far as radioactivity is concerned.

Statistical inference tests (see Table 4) show that the two IRL units (ES-1 and ES-2) could be considered as belonging to one and the same parent population from the radioactivity point of view (so they are coded as ES). The normal probability plot (see Fig. 8g) proves that this new IRL unit (ES), which comes from adding the aeroradiometric measurements of ES-1 and ES-2 shows normal distribution.

Samr El-Qaa Formation (CQ)

According to the geological map of the area under study (see Fig. 2), Samr El-Qaa (CQ) formation is exposed in only one locality. As a result of the application of the statistical methods of analysis on the aerial total-count radiometric survey data, this unit is considered as one IRL unit coded as CQ (see Fig. 10). The normal probability plot (see Fig. 8h) and the chi-square test value (see Table 2) demonstrate that the measurements registered over this IRL unit are normally distributed.

Wadi Qena Formation (KLQ)

According to the geological map (see Fig. 2) of the study area, Wadi Qena Formation (KLQ) is located in three localities in its western part. As a result of the application of the statistical methods of analysis for the total-count aerial radiometric survey data, the Wadi Qena Formation was treated as three independent IRL units (KLQ-1, KLQ-2 and KLQ-3, Fig. 8). The normal probability plots (see Fig. 8i, 8j & 8k) and the chi-square test values (see Table 2) prove that only the measurements recorded over KLQ-1 IRL unit are not normally distributed.

Statistical inference tests were applied to the computed statistical characteristics of the two IRL units, which showed normal distributions (KLQ-2 and KLQ-3). The results of these two tests are organized in Table 4. From the results of the application of the two statistical inference tests, a conclusion could be reached that these two IRL units could be considered as belonging to one and the same parent population as far as the T.C. aerial radioactivity is considered. Thus, they are coded as KLQ-2. The normal probability plot (see Fig. 8l) and the chi-square test value (see Table 2) reveal that this new IRL unit (KLQ-2), which comes from adding the aeroradiometric measurements of KLQ-2 and KLQ-3, shows normal distribution.

Galala Formation (KUG)

According to the geological map (see Fig. 2), the Galala Formation (KUG) is situated in two localities in the western part of the study area. Table 2 shows that the measurements registered over the KUG formation are not normal distributed. As a result of the application of the statistical methods of analysis on the total-count aerial radiometric survey data, the Galala Formation was treated as two independent IRL units (KUG-1 and KUG-2). The normal probability plots (see Figs. 9a & 9b) and the chi-square test values of both of these two IRL units show that their measurements show normal distribution (see Table 2).

From the results of the application of the Fisher's (F-) statistical inference test (see Table 4), a conclusion could be reached that these two IRL units could not be considered as belonging to one and the same parent population as far as the T.C. aerial radioactivity is concerned.

Undifferentiated Quaternary Sediments (QW)

According to the geological map (see Fig. 2) of the study area, the undifferentiated Quaternary sediments (QW) are situated in four localities. Their calculated arithmetic means range from 4.35 to 13.55Ur and their standard deviations vary from 0.67 to 4.61Ur (see Table 2). As a result of the application of the statistical methods analysis for the aerial total-count radiometric survey data, these sediments were treated as four IRL units (QW-1, QW-2, QW-3 and QW-4). The normal probability plots (see Figs. 9c, 9d, 9e & 9f) and the chi-square test values (see Table 2) demonstrate that, only the measurements recorded over QW-3 IRL unit show abnormal distribution.

Statistical inference tests were applied to see what relations may arise among the three various and normal IRL units (QW-1, QW-2, and QW-4). This work has been achieved by applying the Bartlett's test for comparison of their variances as one group, as well as the Fisher's (F-) test for comparison of their variances as three pairs of IRL units. The results of these two statistical inference tests (see Tables 3 and 4) show that the three measurements recorded over normal IRL units of the undifferentiated Quaternary sediments could not be considered as belonging to one and the same parent population as far as the T.C. aerial radioactivity is concerned.

The resultant interpreted radiolithologic unit (IRLU) map (see Fig. 10) and the detailed graph showing the variation of the arithmetic means (X) of aeroradiospectrometric data of the different interpreted radiometric lithologic (IRL) units (Fig. 11) of the area under investigation were drawn.

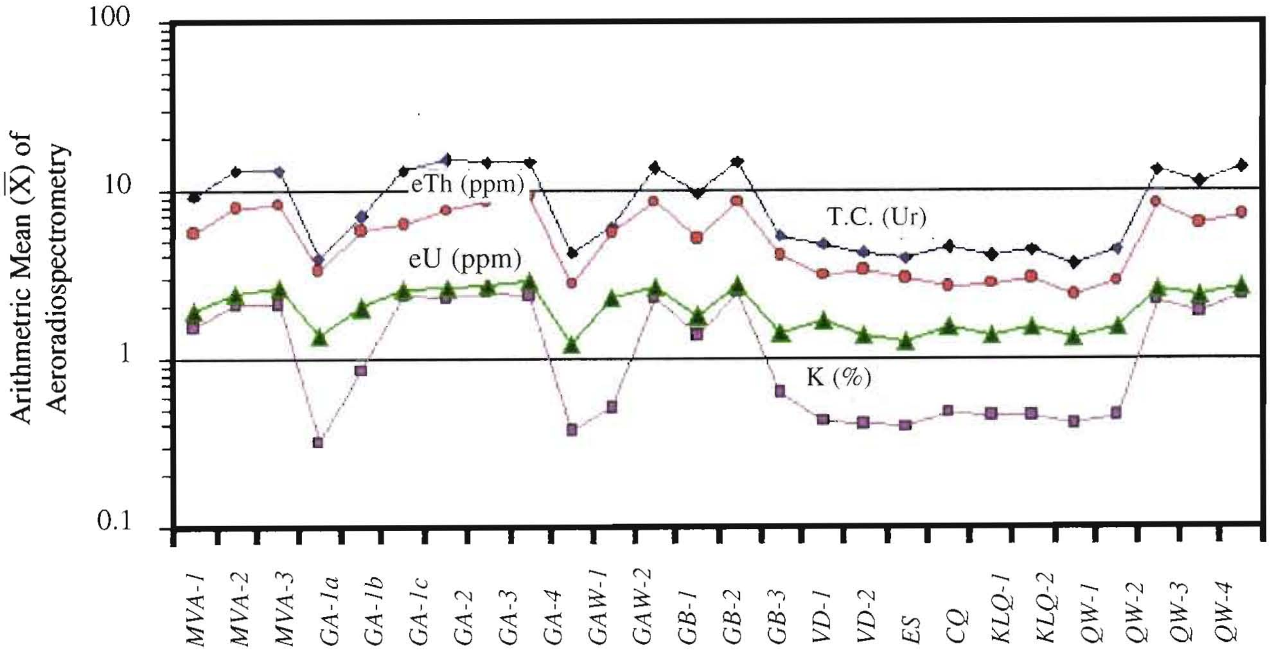

Fig. 11: Detailed graphs showing the variation of the arithmetic means (X) of aeroradiospectrometric data (Table 4) of the different interpreted radiometric lithologic (IRL) units (Fig. 10), Gabal Um Rabul area, Northern Eastern Desert, Egypt.

Conclusions

The geological and aeroradiospectrometric maps were considered as bases for the radiometric lithologic interpretation of the false-coloured contour and image maps of the Gabal Um Rabul area, Northern Eastern Desert, Egypt. Meanwhile, the interpreted radiometric lithologic unit (IRLU) map is regarded as the resultant lithological configuration of the investigated area, according to the computed aerial radiospectrometric characteristics of each IRL unit. Some of the lithologically-mapped rock units were divided into two or more subunits according to their aerial radiospectrometric identities, which express their content of radioactive elements included in the radioactive minerals.

The correlation between aeroradiospectrometry and lithology was conducted in two ways: the first took into consideration the original lithological units, while the latter took into account the IRL units. The latter (IRLU) map (see Fig. 10) was the final result of modification of the first geological map (see Fig. 2), on the basis of the results of statistical analysis applied to airborne radiospectrometric survey data, and in view of the differences in the aerial radiospectrometric levels and patterns.

By testing the homogeneity of measurements recorded over the study area as a whole, the computed values of the (χ^2) test, the normal probability plot (NPP), and the frequency histogram (FH), all indicate that they are not homogeneous. The previous tests all indicated that the area under investigation is not representing one lithologic unit as a whole, but contains different types of rock units, a conclusion that is true.

Four various statistical inference tests were applied to the computed aerial total-count (T.C.) radiometric characteristic statistics to determine whether or not a statistically significant difference exists between the computed statistics (arithmetic means and standard deviations) for the different IRL units (normal distributions) in the area under consideration.

The differential statistical analysis of the aerial radiospectrometric survey data recorded over the various IRL units (see Fig. 11) showed that the area under study possesses a wide range of spectral radioactivity. It changes in total-count radioactivity from less than 4.0 Ur over the sedimentary rocks to more than 32.0 Ur over a zone located on the geologically-mapped older granites, from less than 0.2 % K over sedimentary rocks to more than 3.2 % K over a zone located on the so-mapped older granites, from about 0.5 ppm eU over sedimentary rocks to more than 7.5 ppm eU over a zone located on the so-mapped older (?) granites and from less than 2.0 ppm eTh over sedimentary rocks to more than 28.0 ppm eTh over a zone located on the so-mapped older granites. This very high zone is believed to correspond with younger granites rather than older granites, and so it represents an error in the geological mapping.

The resultant radiolithologic unit (IRLU) map (see Fig. 10) and the detailed graph of the variation of the arithmetic means (see Fig. 11) show that, the study area contains four basement rock units with different T.C. radiometric levels and different radioelement concentrations:

*__metavolcanics__ (11.9Ur, 1.9% K, 2.3ppm eU and 7.3ppm eTh).

*__older granites__ (9.95Ur, 1.4% K, 2.2ppm eU and 6.1ppm eTh).

*__younger granites__ (12.6Ur, 2.0 % K, 2.4ppm eU and 7.4ppm eTh).

*__Dokhan volcanics__ (5.1Ur, 0.5% K, 1.5ppm eU and 3.6ppm eTh).

In addition, the IRLU map (see Fig. 10) includes five sedimentary formations with different T.C. radiometric levels and different radioelement concentrations:

*__Araba Formation__ (4.3Ur, 0.4% K, 1.3ppm eU and 3.3ppm eTh).

*__Samr El-Qaa Formation__ (3.9Ur, 0.3% K, 1.2ppm eU and 2.9ppm eTh).

*__Wadi Qena Formation__ (3.95Ur, 0.4% K, 1.5ppm eU and 2.7ppm eTh).

*__Galala Formation__ (4.1Ur, 0.46% K, 1.35ppm eU and 2.8ppm eTh).

*__Quaternary sediments__ (10.6Ur, 1% K, 2.3ppm eU and 6.0ppm eTh).

The radio-spectrometric characteristics of these radiolithologic units can be tabulated as follows: (Table 5)

Table 5: Radio-spectrometric characteristics of radiolithologic units

Radiolithologic units	T.C in Ur	K, in %	eU, in ppm	eTh, in ppm
Basement rocks				
1 - Metavolcanics	11.9	1.9	2.3	7.3
2 - Older granites	10.0	1.4	2.2	6.1
3 - Younger granites	12.6	2.0	2.4	7.4
4 - Dokhan volcanics	5.1	0.5	1.5	3.6
Sedimentary Formations				
1 - Araba formation	4.3	0.4	1.3	3.3
2 - Samr-El-Qaa formation	4.0	0.4	1.3 3.0	
3 - Wadi-Qena formation	4.6	0.4	1.5	2.7
4 - Galala formation	4.1	0.5	1.4	2.8
5 - Quaternary sediments	10.6	1.7	2.3	6.0

References

Abdellah, A. M., Darwish, M., El-Aref, M., and **Helba, A. (1992)** Lithogstratigraphy of the Pre-Cambrian clastics in north Wadi Qena, Eastern Desert, Egypt. *Proceedings of the Conference on the Geology of the Arab World* (GAW). Cairo University, Giza, Egypt.

Aero-Service (1984) *Final operational report of airborne magnetic/radiation survey in the Eastern Desert, Egypt,* Volumes 1.-.6. Conducted for the Egyptian General Petroleum Corporation (EGPC) and the Egyptian Geological Survey and Mining Authroty (EGSMA). Aero-Service Division, Western Geophysical Company, Houston, Texas, USA.

Ammar, A. A., Meleik, M. L., and **Fouad, K. M.** (1982) The aerial radiometric identification of granitic plutons by statistical analysis. *Computers & Geosciences* **8** (2): 209-219.

CONOCO Inc. (1987) *Geological map of Egypt.* Scale 1:500,000, -NH36SW- Beni Suef, Egypt.

CONOCO Inc. (1989) Stratigraphic lexicon and explanatory notes to the geological map of Egypt, Scale 1:500,000. Edited by Maurice Hermina, Eberhard Klitzsch and Franz K. List.

Darnley, A. G. (1973) Airborne gamma-ray survey techniques: present and future. In: **Uranium Exploration Methods,** *Proceedings of a Panel of the International Atomic Energy Agency (IAEA).* Vienna, Austria, 67-108 pp.

Darnely, A. G., and **Ford, K. L.** (1989) Regional airborne gamma ray survey: A review. *Proceedings of Exploration' 87: Third Decennial International Conference on Geophysical and Geochemical Exploration for Minerals and Groundwater,* Vol. **II**. Geol. Surv. of Canada, Ontario.

Darnely, A. G. and **Grasty, R. L.** (1971) Mapping from the air by gamma-ray spectrometry. *Third International Geochemical Symposium,* Vol. II. Can. Inst. Min. Met., Toronto, Canada, 485-500 pp.

Duval, J. S. (1983) Computer images of aerial gamma-ray spectrometric data. *Geophysics* **48** (16): 722-735 pp

El-Ramly, M. F., Bodanov, V. I., and **Hussein, A. A.** (1971) The alkaline rocks of Southern Eastern Egypt. *Geol. Surv. Egypt,* Paper No. 53, pp. 111-115.

El-Sadek, M. A. (1998) *Airborne spectrometry and magnetometry of Wadi Araba area, Northern Eastern Desert, Egypt, in supporting of geological mapping and mineral exploration.* Ph. D. Thesis, Fac. of Science, Ain Shams Univ., Cairo, Egypt (unpublished).

International Atomic Energy Agency (IAEA) (1988) Geochemical exploration for uranium. *IAEA Technical Report Series,* No. 284, Vienna, Austria.

Killeen, P. G. (1979) Gamma ray spectrometric methods in uranium exploration and interpretation. *In:* **Hood, Peter J. (ed.)** *Geophysics and Geochemistry in the Search for Metallic Ores.* Geological Survey of Canada. Economic Geology Report, No. **31**, 163-229 pp.

Klitzsch, E., List, F. K., Pohlmann, G., Handley, R., Hermina, M. and **Meissner, B., (eds.)** (1986 & 1987) Geological Map of Egypt, Scale 1:500,000 (20 sheets). CONOCO/E.G.P.C., Cairo, Egypt.

Mendenhall, W., and **Sincich, T.** (1992) *Statistics for engineering and sciences,* 3rd ed. Maxwell Macmillan International Editions.

Ref. 2166
Received 21/04/2002
In revised form 26/12/2002